Comput. Methods Appl. Mech. Engrg. 199 (2010) 841–852

Contents lists available at ScienceDirect

Comput. Methods Appl. Mech. Engrg.

journal homepage: www.elsevier.com/locate/cma

Numerical studies of finite element variational multiscale methods for turbulent flow simulations ☆

Volker John *, Adela Kindl

FR 6.1 – Mathematik, Universität des Saarlandes, Postfach 15 11 50, 66041 Saarbrücken, Germany

ARTICLE INFO

Article history:
Received 27 December 2007
Received in revised form 21 July 2008
Accepted 8 January 2009
Available online 22 January 2009

Keywords:
Variational multiscale methods
Finite element methods
Turbulent channel flow
Residual free bubble functions

ABSTRACT

Different realizations of variational multiscale (VMS) methods within the framework of finite element methods are studied in turbulent channel flow simulations. One class of VMS methods uses bubble functions to model resolved small scales whereas the other class contains the definition of the resolved small scales by an explicit projection in its set of equations. All methods are employed with eddy viscosity models of Smagorinsky type. The simulations are performed on grids for which a Direct Numerical Simulation blows up in finite time.

1. Introduction

The simulation of many processes in nature and industry requires as a subtask the simulation of turbulent incompressible flows. Incompressible flows are modeled by the incompressible Navier–Stokes equations, which read in dimensionless form

$$\begin{aligned} &\mathbf{u}_t - 2\nu\nabla\cdot\mathbb{D}(\mathbf{u}) + (\mathbf{u}\cdot\nabla)\mathbf{u} + \nabla p = \mathbf{f} \quad \text{in } (0,T)\times\Omega,\\ &\nabla\cdot\mathbf{u} = 0 \quad \text{in } [0,T]\times\Omega,\\ &\mathbf{u}(0,\mathbf{x}) = \mathbf{u}_0 \quad \text{in } \Omega, \end{aligned} \tag{1}$$

where $\mathbf{u}(t,\mathbf{x})$ denotes the fluid velocity, $\mathbb{D}(\mathbf{u}) = (\nabla\mathbf{u} + \nabla\mathbf{u}^T)/2$ is the velocity deformation tensor, $p(t,\mathbf{x})$ is the fluid pressure, T is the simulation time, and $\Omega \subset \mathbb{R}^3$ is a spatial domain. The parameter $\nu > 0$ is the kinematic viscosity, and $\mathbf{f}(t,\mathbf{x})$ represents the external body force (e.g. gravity). The initial velocity field $\mathbf{u}_0$ is assumed to be divergence-free. The equations (1) have to be closed with appropriate boundary conditions.

Turbulent flows are characterized by a wide spectrum of sizes of the flow structures (scales) ranging from large ones to very small ones. In general, most of the small scales cannot be even represented on grids of the underlying discretization of the Navier–Stokes equations. Consequently, these scales cannot be simulated. However, they are essential for the turbulent character of the flow (energy cascade) and neglecting them in the simulations would lead to laminar results (which are of course wrong). The difficult task consists in modeling the influence of these unresolved (small, fine) scales onto the resolved scales, which is called turbulence modeling. There are many ideas and approaches for turbulence modeling, to mention only two popular ones, the k–ε model [1] and the (traditional) Large Eddy Simulation (LES) [2]. A comparatively new approach are variational multiscale (VMS) methods which posses similarities but also fundamental differences to the traditional LES.

VMS methods are based on general ideas for the simulation of multiscale phenomena from [3,4]. The first presentation of these ideas in connection with turbulent flows can be found in [5] and the first numerical results were published around the same time in [6,7]. Meanwhile, one can distinguish several classes of VMS methods. However, they are all based on two fundamental features:

- VMS methods use a variational form of the underlying equation which is formulated in appropriate function spaces.
- The scales are defined by projections into subspaces.

These two features distinguish VMS methods from traditional LES approaches. Traditional LES methods are based on a strong form of the underlying equation and the large scales are defined by spatial averaging (filtering). This way of defining the large scales leads to difficulties in the rigorous mathematical analysis of LES models for flows in bounded domains since always additional terms arise from the necessary commutation of the filter operator and the spatial differential operators. These additional terms are neglected in practice resulting in so-called commutation errors. It

☆ The research of A. Kindl was supported by the Deutsche Forschungsgemeinschaft (DFG) by Grants No. Jo 329/7-1 and No. Jo 329/7-2.

* Corresponding author. Tel.: +49 681 302 2784; fax: +49 681 302 4443.
E-mail addresses: john@math.uni-sb.de (V. John), adela@c-kindl.de (A. Kindl).

0045-7825/$ - see front matter © 2009 Elsevier B.V. All rights reserved.
doi:10.1016/j.cma.2009.01.010

has been shown analytically that these errors are not negligible on the boundary and in a vicinity of the boundary [8–11]. We think that the definition of scales in the way of VMS methods is more appropriate, at least from the mathematical point of view. For instance, in [12,13] the commutation between the projection operator defining the large scales in certain VMS methods and spatial differential operators has been shown.

Apart from the two fundamental properties given above, the available proposals of VMS methods are quite different. We will concentrate here on finite element VMS (FEVMS) methods. VMS methods based on other discretizations can be found, for instance, in [6,7,13–16]. The FEVMS method proposed in the pioneering paper [5] is based on a two-scale decomposition of the flow field into large scales $(\bar{\mathbf{u}}, \bar{p})$ and small scales $(\hat{\mathbf{u}}, \hat{p})$. A finite dimensional space is used for defining the large scales and consequently, the dimension of the space for the small scales is infinite. After the decomposition of the flow field, a variational form of the Navier–Stokes equations (1) can be written as a coupled system of two sets of equations, one with the test functions from the large scale space and the other one with the test functions from the small scale space. The second set consists of infinitely many equations. In [5], for finite element methods, it was proposed to approximate the infinite dimensional small scale space with local, higher order polynomials, so-called bubble functions, which model the so-called resolved small scales. In addition, the influence of the scales which are not resolved by the bubble functions is modeled with an eddy viscosity model. This eddy viscosity model acts directly only on the bubble functions. To our knowledge, numerical simulations with this form of a FEVMS method cannot be found so far in the literature. This method will be studied in the present paper and its shortcomings will be addressed.

In [17–19], a FEVMS method based on the initial proposal from [5] was developed and studied. In addition to using bubble functions for the resolved small scale velocity and an eddy viscosity model which accounts for the influence of the unresolved scales onto the resolved small scales, the resolved small scale pressure is modeled by the residual of the large scale continuum equation, see [20] for a motivation of this modeling in the context of the Stokes equations. This model leads to a well-known stabilization term in the large scale equations, the so-called grad–div stabilization [21,22]. FEVMS methods of this type are included in the numerical studies presented in this paper. In Sections 2.2, 2.3 a derivation of the bubble-based FEVMS methods is presented which uses the bubble finite element spaces from the beginning. This way, the bubble-based FEVMS methods are derived on the basis of a three-scale decomposition of the flow field into large, resolved small and unresolved scales [23].

There is another class of FEVMS methods in which the scale separation relies on the polynomial degree of finite element functions [24,25]. In [24], continuous finite elements were used with a hierarchical basis whereas in [25] discontinuous finite elements were applied. In both FEVMS methods, the large scales are defined by the low order polynomials and the resolved small scales by the higher order polynomials.

A proposal of a FEVMS method based on a three-scale decomposition of the flow field can be found in [12]. A main feature of this method is the use of standard finite element spaces for all resolved scales. The separation of the large scales and the resolved small scales is achieved with an additional large scale space. An equation defining the projection into this space is explicitly contained in this method. This projection-based three-scale FEVMS method adds an additional viscous term for the resolved small scales to the finite element momentum equation of the Navier–Stokes equations. The parameter in this term is generally chosen to be an eddy viscosity model of Smagorinsky-type [12,26,27]. The ideas of this projection-based VMS method can also be applied in the framework of finite volume discretizations [13]. Some variants of the projection-based FEVMS method are considered in the numerical studies, see Section 2.4.

The philosophy of the three-scale VMS methods resembles the philosophy of the dynamic Smagorinsky LES model [28,29]. In this LES model, the parameter in the Smagorinsky eddy viscosity term is adjusted dynamically to reduce the viscosity of the model in regions were it is not needed. In the three-scale VMS methods, the reduction of the viscosity is achieved by applying the Smagorinsky model only to the resolved small scales, whose definition depends on the current solution.

The last VMS method which will be mentioned in some detail further on in the introduction was proposed quite recently in [30]. It is based on a two-scale decomposition of the flow field achieved via a projection operator [31]. By writing a variational form of the Navier–Stokes equations as a coupled system with test functions from the large and the small scale subspaces, respectively, it is readily shown that the small scales can be formally represented as an unknown functional of the residual of the large scales. To approximate this functional, the small scales are expressed as a perturbation series where the perturbation parameter is an appropriate norm of the large scale residual. For the unknown terms of this perturbation series, a recursive system of equations can be derived where the left hand side in all equations has the form of a linearized Navier–Stokes equations. Thus, the solution of these equations can be formally expressed with an appropriate Green's operator, the so-called fine-scale Green's operator. In [31], it has been shown that the fine-scale Green's operator can be expressed using the classical Green's operator and the projection defining the scale separation. To obtain a numerical method, in [30] it is proposed to truncate the perturbation series after the first term and to approximate the fine-scale Green's operator. Altogether, the small scales are modeled in [30] to be proportional to the residual of the large scales. Inserting this model into the equations with the large scale test functions, one obtains a generalization of the well-known streamline-upwind Petrov–Galerkin (SUPG) method for the Navier–Stokes equations. Besides the SUPG term and the grad–div term, additional terms arise which can be interpreted as the cross stresses and the Reynolds stresses known from the traditional LES. The two-scale VMS method from [30] does not use an eddy viscosity model. However, there is some freedom in choosing the parameters in the additional terms. This quite new method is not yet included in the numerical studies presented in this paper.

This paper will present numerical studies at turbulent channel flows at $Re_\tau = 180$ and $Re_\tau = 395$. Numerical studies of turbulence models at academic test examples may have different goals. One goal might be to use resolutions (grids) which are sufficiently fine compared with the Reynolds number such that an underresolved Direct Numerical Simulation (DNS) can be performed and to show that statistics of the flows are captured better if a turbulence model is applied. Another goal might be to apply turbulence models on grids where a DNS blows up in finite time. In this situation, the use of a turbulence model is necessary in order to perform any simulations at all. The latter case is more likely in applications and it will be considered in this paper. Thus, simulations on rather coarse grids, compared with the Reynolds number, will be presented, which study and compare bubble-based FEVMS methods and some variants of the projection-based FEVMS method. To our best knowledge, a comparison of these methods is so far not available.

The paper is organized as follows. Section 2 contains a detailed description of all considered FEVMS methods. The numerical tests for the channel flow problems are presented in Section 3. Finally, Section 4 summarizes the conclusions and gives an outlook.

2. Finite element variational multiscale methods

This section contains a rather detailed presentation of the studied methods. It has been shown for turbulent channel flow problems that even tiny changes in the data or algorithms eventually lead to large changes in the instantaneous flow fields [32]. The changes in mean values and statistics are less significant. Nevertheless, in view of the sensitivity of the turbulent channel flow to small perturbations, it seems important to us to give at least a detailed description of the main algorithms and methods which were used in the numerical studies.

Throughout this paper, standard notations for Lebesgue and Sobolev spaces are used, e.g. see [33]. The inner product in $(L^2(\Omega))^d$, $d \in \mathbb{N}$, is denoted by $(\cdot,\cdot)$.

2.1. Basic discretizations and linearization scheme

For simplicity of presentation, we consider in this section no-slip boundary conditions $\mathbf{u} = \mathbf{0}$ on $[0,T]\times\partial\Omega$. The Crank–Nicolson discretization of the time derivative of the velocity in the Navier–Stokes equations (1) is the first step in our discretization approach. Let t_k be the current discrete time and Δt_k be the time step from t_{k-1} to t_k. To compute the solution $(\mathbf{u}_k, p_k) := (\mathbf{u}(t_k), p(t_k))$ of the Navier–Stokes equations at t_k, the following set of equations has to be solved

$$\begin{aligned}
&\mathbf{u}_k + 0.5\Delta t_k[-2\nu\nabla\cdot\mathbb{D}(\mathbf{u}_k) + (\mathbf{u}_k\cdot\nabla)\mathbf{u}_k] + \Delta t_k\nabla p_k \\
&\quad = \mathbf{u}_{k-1} - 0.5\Delta t_k[-2\nu\nabla\cdot\mathbb{D}(\mathbf{u}_{k-1}) + (\mathbf{u}_{k-1}\cdot\nabla)\mathbf{u}_{k-1}] \\
&\qquad + 0.5\Delta t_k\mathbf{f}_{k-1} + 0.5\Delta t_k\mathbf{f}_k \quad \text{in } \Omega, \\
&\nabla\cdot\mathbf{u}_k = 0 \quad \text{in } \Omega.
\end{aligned} \tag{2}$$

Note that the temporal discretization is only applied to the velocity, see [8] for a discussion of this issue.

Next, (2) is transformed into a variational form by multiplying the equations with appropriate test functions and applying integration by parts. A variational form of (2) reads as follows: Find $(\mathbf{u}_k, p_k) \in V\times Q := (H_0^1(\Omega))^3 \times L_0^2(\Omega)$ such that

$$\begin{aligned}
&(\mathbf{u}_k,\mathbf{v}) + 0.5\Delta t_k[(2\nu\mathbb{D}(\mathbf{u}_k),\mathbb{D}(\mathbf{v})) + ((\mathbf{u}_k\cdot\nabla)\mathbf{u}_k,\mathbf{v})] - \Delta t_k(p_k,\nabla\cdot\mathbf{v}) \\
&\quad = (\mathbf{u}_{k-1},\mathbf{v}) - 0.5\Delta t_k[(2\nu\mathbb{D}(\mathbf{u}_{k-1}),\mathbb{D}(\mathbf{v})) + ((\mathbf{u}_{k-1}\cdot\nabla)\mathbf{u}_{k-1},\mathbf{v})] \\
&\qquad + 0.5\Delta t_k(\mathbf{f}_{k-1},\mathbf{v}) + 0.5\Delta t_k(\mathbf{f}_k,\mathbf{v}), \\
&0 = (\nabla\cdot\mathbf{u}_k, q)
\end{aligned} \tag{3}$$

for all $(\mathbf{v},q)\in V\times Q$.

This is a nonlinear problem in the discrete time t_k, which is solved by a fixed point iteration. Given $\mathbf{u}_k^{(0)} = \mathbf{u}_{k-1}$, compute $(\mathbf{u}_k^{(l)}, p_k^{(l)}) \in V\times Q$ such that

$$\begin{aligned}
&(\mathbf{u}_k^{(l)},\mathbf{v}) + 0.5\Delta t_k\left[(2\nu\mathbb{D}(\mathbf{u}_k^{(l)}),\mathbb{D}(\mathbf{v})) + ((\mathbf{u}_k^{(l-1)}\cdot\nabla)\mathbf{u}_k^{(l)},\mathbf{v})\right] \\
&\quad - \Delta t_k(p_k^{(l)},\nabla\cdot\mathbf{v}) \\
&\qquad = (\mathbf{u}_{k-1},\mathbf{v}) - 0.5\Delta t_k[(2\nu\mathbb{D}(\mathbf{u}_{k-1}),\mathbb{D}(\mathbf{v})) + ((\mathbf{u}_{k-1}\cdot\nabla)\mathbf{u}_{k-1},\mathbf{v})] \\
&\qquad\quad + 0.5\Delta t_k(\mathbf{f}_{k-1},\mathbf{v}) + 0.5\Delta t_k(\mathbf{f}_k,\mathbf{v}), \\
&0 = (\nabla\cdot\mathbf{u}_k^{(l)}, q)
\end{aligned} \tag{4}$$

for all $(\mathbf{v},q)\in V\times Q$, for $l = 1,2,\ldots$. The linear equations (4) are discretized in space by an inf–sup stable finite element method with second order velocity and first order pressure.

The Crank–Nicolson scheme, inf–sup stable finite element methods and the fixed point iteration are also the basic components of the FEVMS methods presented below. The motivation for using these components comes from our own experiences. Numerical studies, e.g. [34,35], show that one has to use a second order time-stepping scheme for computing accurate results in incompressible flow simulations. Similarly, finite element methods with second order velocity and first order pressure are in general much more accurate than lower order methods [36,34]. Finally, numerical studies in [37] have shown that the application of a fixed point iteration is more efficient than using Newton's method.

2.2. The bubble-based FEVMS method

This section presents the main ideas and assumptions of a bubble-based FEVMS method. A close connection between the philosophy of VMS methods and the use of residual-free bubble stabilizations was established in [38]. Under the assumption that the small scale phenomena exists only in the interior of the mesh cells, it was shown that both approaches are equivalent. The principal idea of using bubble functions for the scale separation in FEVMS methods for turbulent flows was pointed out in [5]. We will give a short derivation of the method which starts, in contrast to [5], with the space of bubble functions and a three-scale decomposition of the flow field.

Let $V = \overline{V}\oplus\widetilde{V}\oplus\widehat{V}$, $Q = \overline{Q}\oplus\widetilde{Q}\oplus\widehat{Q}$ be a decomposition of the spaces V and Q into large scales, resolved small scales and unresolved small scales. Accordingly, all functions can be decomposed, e.g. the velocity $\mathbf{u}_k = \bar{\mathbf{u}}_k + \tilde{\mathbf{u}}_k + \hat{\mathbf{u}}_k$, $\mathbf{v} = \bar{\mathbf{v}} + \tilde{\mathbf{v}} + \hat{\mathbf{v}}$.

A bubble-based FEVMS method can be derived by first decomposing the test functions in (4) and writing (4) as a coupled system for the large scale, resolved small scale and unresolved scale test functions. In this step, only the linearity of (4) with respect to the test functions is important. Then, the following ideas and assumptions are used, see [39] for more details:

- neglect the equation with the unresolved scale test functions since these test functions are not available,
- assume that the direct influence of the unresolved scales onto the large scales can be neglected, i.e. neglect all terms in the equations for the large scales where unresolved scales occur,
- model the influence of the unresolved scales onto the resolved small scales by means of a turbulence model, e.g. an eddy viscosity model of Smagorinsky-type.

At the discrete time t_k, these assumptions lead to the following system of coupled equations: Find $(\bar{\mathbf{u}}_k,\bar{p}_k)\times(\tilde{\mathbf{u}}_k,\tilde{p}_k)\in(\overline{V}\times\overline{Q})\times(\widetilde{V}\times\widetilde{Q})$ such that a large scale equation

$$\begin{aligned}
&(\bar{\mathbf{u}}_k,\bar{\mathbf{v}}) + 0.5\Delta t_k[(2\nu\mathbb{D}(\bar{\mathbf{u}}_k),\mathbb{D}(\bar{\mathbf{v}})) + ((\bar{\mathbf{u}}_k\cdot\nabla)\bar{\mathbf{u}}_k,\bar{\mathbf{v}})] - \Delta t_k(\bar{p}_k,\nabla\cdot\bar{\mathbf{v}}) \\
&\quad = (\mathbf{u}_{k-1},\bar{\mathbf{v}}) - 0.5\Delta t_k[(2\nu\mathbb{D}(\mathbf{u}_{k-1}),\mathbb{D}(\bar{\mathbf{v}})) + ((\mathbf{u}_{k-1}\cdot\nabla)\mathbf{u}_{k-1},\bar{\mathbf{v}})] \\
&\qquad - (\tilde{\mathbf{u}}_k,\bar{\mathbf{v}}) - 0.5\Delta t_k[(2\nu\mathbb{D}(\tilde{\mathbf{u}}_k),\mathbb{D}(\bar{\mathbf{v}})) + ((\mathbf{u}_k\cdot\nabla)\tilde{\mathbf{u}}_k,\bar{\mathbf{v}}) \\
&\qquad + ((\tilde{\mathbf{u}}_k\cdot\nabla)\bar{\mathbf{u}}_k,\bar{\mathbf{v}})] + \Delta t_k(\tilde{p}_k,\nabla\cdot\bar{\mathbf{v}}) \\
&\qquad + 0.5\Delta t_k(\mathbf{f}_{k-1},\bar{\mathbf{v}}) + 0.5\Delta t_k(\mathbf{f}_k,\bar{\mathbf{v}}), \\
&(\nabla\cdot\bar{\mathbf{u}}_k,\bar{q}) = -(\nabla\cdot\tilde{\mathbf{u}}_k,\bar{q})
\end{aligned} \tag{5}$$

for all $(\bar{\mathbf{v}},\bar{q})\in\overline{V}\times\overline{Q}$ and a resolved small scale equation

$$\begin{aligned}
&(\tilde{\mathbf{u}}_k,\tilde{\mathbf{v}}) + 0.5\Delta t_k[(2\nu+\nu_T)\mathbb{D}(\tilde{\mathbf{u}}_k),\mathbb{D}(\tilde{\mathbf{v}})) + ((\mathbf{u}_k\cdot\nabla)\tilde{\mathbf{u}}_k,\tilde{\mathbf{v}})] \\
&\quad - \Delta t_k(\tilde{p}_k,\nabla\cdot\tilde{\mathbf{v}}) \\
&\qquad = (\mathbf{u}_{k-1},\tilde{\mathbf{v}}) - 0.5\Delta t_k[(2\nu\mathbb{D}(\mathbf{u}_{k-1}),\mathbb{D}(\tilde{\mathbf{v}})) + ((\mathbf{u}_{k-1}\cdot\nabla)\mathbf{u}_{k-1},\tilde{\mathbf{v}})] \\
&\qquad\quad - (\bar{\mathbf{u}}_k,\tilde{\mathbf{v}}) - 0.5\Delta t_k[(2\nu\mathbb{D}(\bar{\mathbf{u}}_k),\mathbb{D}(\tilde{\mathbf{v}})) + ((\mathbf{u}_k\cdot\nabla)\bar{\mathbf{u}}_k,\tilde{\mathbf{v}})] \\
&\qquad\quad + \Delta t_k(\bar{p}_k,\nabla\cdot\tilde{\mathbf{v}}) + 0.5\Delta t_k(\mathbf{f}_{k-1},\tilde{\mathbf{v}}) + 0.5\Delta t_k(\mathbf{f}_k,\tilde{\mathbf{v}}), \\
&(\nabla\cdot\tilde{\mathbf{u}}_k,\tilde{q}) = -(\nabla\cdot\bar{\mathbf{u}}_k,\tilde{q})
\end{aligned} \tag{6}$$

for all $(\tilde{\mathbf{v}},\tilde{q})\in\widetilde{V}\times\widetilde{Q}$ have to be solved.

In (6), the term $(\nu_T\mathbb{D}(\tilde{\mathbf{u}}_k),\mathbb{D}(\tilde{\mathbf{v}}))$ models the influence of the unresolved scales onto the resolved small scales by means of an eddy viscosity turbulence model. Possible candidates are Smagorinsky-type models [40] of the form

$$\nu_T = C_S h_K^2\|\mathbb{D}(\tilde{\mathbf{u}})\|_F, \tag{7}$$

$$\nu_T = C_S h_K^2\|\mathbb{D}(\bar{\mathbf{u}})\|_F, \tag{8}$$

$$\nu_T = C_S h_K^2\|\mathbb{D}(\bar{\mathbf{u}}+\tilde{\mathbf{u}})\|_F. \tag{9}$$

Following [6,7], the models in (7)–(9) are called small–small, large–small and all–small. Here, C_S is a user-chosen constant, h_K is an appropriate measure of the mesh cell K and $\|\cdot\|_F$ is the Frobenius norm of a tensor.

In a bubble-based FEVMS method, standard finite element spaces are used for the large scales $\overline{V} \times \overline{Q} = \overline{V}^h \times \overline{Q}^h$. The finite element spaces for the resolved small scales require a higher resolution than the finite element spaces for the large scales. This can be achieved in various ways: by using higher order finite elements, by refining the given grid or by combining these approaches. However, the result of all approaches is that the solution of the resolved small scale equations (6) would be much more expensive than solving the large scale equations (5). This will be circumvented in a bubble-based FEVMS method by considering (6) in the space of residual-free bubble functions for the velocity. A bubble function is a function from $H_0^1(\Omega)$ whose support is only one mesh cell and which vanishes on the faces of this mesh cell. With these functions, the solution of (6) can be localized. In the space of residual-free bubbles, a solution is sought which satisfies the strong form of the underlying partial differential equation in the interior of the mesh cells. The space of these bubble functions is infinite dimensional and it will be denoted by $\widetilde{V}_{\text{bub}}$. The use of bubble functions for the stabilization of finite element methods for the Navier–Stokes equations was proposed already in [41].

Usually, simplifying assumptions are made in the definition of the resolved small scales. The first method which will be studied is very close to (5) and (6), with only small modifications. We assume that both $\bar{\mathbf{u}}_k$ and $\tilde{\mathbf{u}}_k$ are discretely divergence-free with respect to the sum of the large scale pressure finite element space and the bubble pressure space. For reasons of efficiency, the gradient form of the viscous term is used in the resolved small scale equations and some right hand side terms in the large scale equations. For the same reason, a linearized version of the resolved small scale equations is solved only once in each discrete time, namely at the beginning using the large scales from the previous discrete time. This gives the following coupled system: Find $(\bar{\mathbf{u}}_k, \bar{p}_k) \times (\tilde{\mathbf{u}}_k, \tilde{p}_k) \in (\overline{V} \times \overline{Q}) \times (\widetilde{V}^h_{\text{bub}} \times \widetilde{Q}^h_{\text{bub}})$ such that

$$
\begin{aligned}
&(\bar{\mathbf{u}}_k, \bar{\mathbf{v}}) + 0.5\Delta t_k[(2\nu\mathbb{D}(\bar{\mathbf{u}}_k), \mathbb{D}(\bar{\mathbf{v}})) + ((\bar{\mathbf{u}}_k \cdot \nabla)\bar{\mathbf{u}}_k, \bar{\mathbf{v}})] - \Delta t_k(\bar{p}_k, \nabla \cdot \bar{\mathbf{v}}) \\
&\quad = (\mathbf{u}_{k-1}, \bar{\mathbf{v}}) - 0.5\Delta t_k[(2\nu\mathbb{D}(\mathbf{u}_{k-1}), \mathbb{D}(\bar{\mathbf{v}})) + ((\mathbf{u}_{k-1} \cdot \nabla)\mathbf{u}_{k-1}, \bar{\mathbf{v}})] \\
&\qquad - (\tilde{\mathbf{u}}_k^{(1)}, \bar{\mathbf{v}}) - 0.5\Delta t_k\Big[(\nu\nabla\tilde{\mathbf{u}}_k^{(1)}, \nabla\bar{\mathbf{v}}) + (((\bar{\mathbf{u}}_{k-1} + \tilde{\mathbf{u}}_k^{(1)}) \cdot \nabla)\tilde{\mathbf{u}}_k^{(1)}, \bar{\mathbf{v}}) \\
&\qquad + ((\tilde{\mathbf{u}}_k^{(1)} \cdot \nabla)\bar{\mathbf{u}}_{k-1}, \bar{\mathbf{v}})\Big] + \Delta t_k(\tilde{p}_k^{(1)}, \nabla \cdot \bar{\mathbf{v}}) \qquad (10) \\
&\qquad + 0.5\Delta t_k(\mathbf{f}_{k-1}, \bar{\mathbf{v}}) + 0.5\Delta t_k(\mathbf{f}_k, \bar{\mathbf{v}}), \\
&(\nabla \cdot \bar{\mathbf{u}}_k, \bar{q}) = 0
\end{aligned}
$$

for all $(\bar{\mathbf{v}}, \bar{q}) \in \overline{V} \times \overline{Q}$ and

$$
\begin{aligned}
&(\tilde{\mathbf{u}}_k^{(1)}, \tilde{\mathbf{v}}) + 0.5\Delta t_k\Big[((\nu + \nu_T)\nabla\tilde{\mathbf{u}}_k^{(1)}, \nabla\tilde{\mathbf{v}}) + ((\mathbf{u}_{k-1} \cdot \nabla)\tilde{\mathbf{u}}_k^{(1)}, \tilde{\mathbf{v}})\Big] \\
&\quad - \Delta t_k(\tilde{p}_k^{(1)}, \nabla \cdot \tilde{\mathbf{v}}) \\
&\quad = (\mathbf{u}_{k-1}, \tilde{\mathbf{v}}) - 0.5\Delta t_k[(\nu\nabla\mathbf{u}_{k-1}, \nabla\tilde{\mathbf{v}}) + ((\mathbf{u}_{k-1} \cdot \nabla)\mathbf{u}_{k-1}, \tilde{\mathbf{v}})] \\
&\qquad - (\bar{\mathbf{u}}_{k-1}, \tilde{\mathbf{v}}) - 0.5\Delta t_k[(\nu\nabla\bar{\mathbf{u}}_{k-1}, \nabla\tilde{\mathbf{v}}) + ((\mathbf{u}_{k-1} \cdot \nabla)\bar{\mathbf{u}}_{k-1}, \tilde{\mathbf{v}})] \\
&\qquad + \Delta t_k(\bar{p}_{k-1}, \nabla \cdot \tilde{\mathbf{v}}) + 0.5\Delta t_k(\mathbf{f}_{k-1}, \tilde{\mathbf{v}}) + 0.5\Delta t_k(\mathbf{f}_k, \tilde{\mathbf{v}}), \qquad (11) \\
&(\nabla \cdot \tilde{\mathbf{u}}_k^{(1)}, \tilde{q}) = 0
\end{aligned}
$$

for all $(\tilde{\mathbf{v}}, \tilde{q}) \in \widetilde{V}^h_{\text{bub}} \times \widetilde{Q}^h_{\text{bub}}$. Here, $\widetilde{V}^h_{\text{bub}}, \widetilde{Q}^h_{\text{bub}}$ denote finite dimensional approximations of $\widetilde{V}_{\text{bub}}, \widetilde{Q}_{\text{bub}}$. The resolved small scale pressure has to be projected into $L_0^2(K)$ for each mesh cell K. In this method, the evolution of the resolved small scales is described in (11). The importance of considering time-dependent subgrid scales was recently pointed out in [42].

The approach (10) and (11) possesses the disadvantage that the solution of the resolved small scales has to be stored. The resolved small scales are defined on a considerably finer grid than the large scales such that the storage overhead becomes non-negligible. Therefore, we studied also a reduced bubble FEVMS method which essentially neglects all terms with the resolved small scales from the discrete time t_{k-1}. That means, $\mathbf{u}_{k-1}$ on the right hand side of the equations for the large scales (10) is replace by $\bar{\mathbf{u}}_{k-1}$. The resolved small scale equations look as follows: Find $(\tilde{\mathbf{u}}_k^{(1)}, \tilde{p}_k^{(1)}) \in \widetilde{V}^h_{\text{bub}} \times \widetilde{Q}^h_{\text{bub}}$ such that

$$
\begin{aligned}
&(\tilde{\mathbf{u}}_k^{(1)}, \tilde{\mathbf{v}}) + \Delta t_k\Big[((\nu + \nu_T)\nabla\tilde{\mathbf{u}}_k^{(1)}, \nabla\tilde{\mathbf{v}}) + ((\bar{\mathbf{u}}_{k-1} \cdot \nabla)\tilde{\mathbf{u}}_k^{(1)}, \tilde{\mathbf{v}})\Big] \\
&\quad - \Delta t_k(\tilde{p}_k^{(1)}, \nabla \cdot \tilde{\mathbf{v}}) \\
&\qquad = -\Delta t_k[(\nu\nabla\bar{\mathbf{u}}_{k-1}, \nabla\tilde{\mathbf{v}}) + ((\bar{\mathbf{u}}_{k-1} \cdot \nabla)\bar{\mathbf{u}}_{k-1}, \tilde{\mathbf{v}}) \\
&\qquad\quad - (\bar{p}_{k-1}, \nabla \cdot \tilde{\mathbf{v}}) - (\mathbf{f}_k, \tilde{\mathbf{v}})], \\
&(\nabla \cdot \tilde{\mathbf{u}}_k^{(1)}, \tilde{q}) = 0 \qquad (12)
\end{aligned}
$$

for all $(\tilde{\mathbf{v}}, \tilde{q}) \in \widetilde{V}^h_{\text{bub}} \times \widetilde{Q}^h_{\text{bub}}$. Neglecting $\tilde{\mathbf{u}}_{k-1}$ leads to a right hand side of the resolved small scale equation which, if $\mathbf{f}_{k-1}$ is in addition replaced with $\mathbf{f}_k$, has the same form as in a backward Euler scheme. For this reason, we also chose the left hand side as in this scheme. The momentum equation for the resolved small scales looks now like for a backward Euler discretization, where the resolved small scales are zero in the previous discrete time.

A remarkable feature of the bubble FEVMS methods is that the left hand side of the large scale Eq. (10) has the same form as for the Galerkin finite element method and that the influence of the turbulence model appears only on the right hand side. It will be shown in Section 3 that this setting still leads to a blow-up of the simulations in finite time.

There is a principal question in all bubble-based FEVMS approaches concerning the physics of the modeling of the resolved small scales. Since these scales are represented by bubble functions, they can move within a mesh cell but they cannot move directly from one mesh cell to another because of the homogeneous Dirichlet boundary conditions on the faces of the mesh cells. The information contained in the resolved small scales can be distributed to other mesh cells only indirectly by the coupling of all resolved scales in the equations for the large scales. This quasi-stationary modeling of the resolved small scales does not reflect the physical reality. However, to our best knowledge, there are no numerical studies available which investigate the impact of this unphysical modeling.

Recently, there have been first proposals for bubble-like methods without homogeneous boundary conditions [43,44]. In [43,44], two-dimensional linear problems without convection were considered and the nonhomogeneous boundary conditions are defined by solutions of ordinary differential equations on the edges of the mesh cells. A straightforward extension of these ideas to three dimensions requires the solution of two-dimensional partial differential equations on the faces of the mesh cells, which seems to be an enormous overhead. In our opinion, the ideas for using bubble-type functions with nonhomogeneous boundary conditions are not yet sufficiently developed to be applicable in turbulent flow simulations.

2.3. The bubble-based FEVMS method with grad–div stabilization

It was shown in [20] for the model problem of the Stokes equation in two dimensions that the P_1/P_1 finite element discretization with residual-free bubble stabilization for both velocity and pressure is equivalent to a residual-based stabilized finite element method. In particular, the resolved small scale pressure bubbles lead to a so-called grad–div stabilization term [21]. The observations from [20] can be used as motivation to model the resolved small scale pressure in the form

$$\tilde{p}_k = -\tau_K(\nabla \cdot \bar{\mathbf{u}}_k), \qquad (13)$$

see also [18,19] for more discussions of this model. This way, the influence of the resolved small scale pressure onto the large scales is not directly taken into account but this influence is modeled. Using (13), $\tilde{p}_k$ vanishes from the resolved small scale equations (6). Since the pressure has vanished, the divergence constraint in (6) is no longer needed and it will be canceled. One obtains a vector-valued equation for $\tilde{\mathbf{u}}_k$. Since there is no longer a divergence constraint for $\tilde{\mathbf{u}}_k$, it does not make sense to have a term with this function in the divergence constraint of the large scale equation (5). The model (13) for the resolved small scale pressure is included into the large scale equation leading to the grad–div term.

As in the bubble FEVMS method, some simplifying assumptions for the resolved small scales are made and we consider a variant with time-dependent resolved small scales and a variant with quasi-static resolved small scales. The bubble-based FEVMS with grad–div stabilization and time-dependent resolved small scales reads as follows: Find $(\bar{\mathbf{u}}_k, \bar{p}_k) \times \tilde{\mathbf{u}}_k \in (\overline{V} \times \overline{Q}) \times \widetilde{V}^h_{\text{bub}}$ such that

$$
\begin{aligned}
&(\bar{\mathbf{u}}_k, \bar{\mathbf{v}}) + 0.5\Delta t_k[(2\nu\mathbb{D}(\bar{\mathbf{u}}_k), \mathbb{D}(\bar{\mathbf{v}})) + ((\bar{\mathbf{u}}_k \cdot \nabla)\bar{\mathbf{u}}_k, \bar{\mathbf{v}})] - \Delta t_k(\bar{p}_k, \nabla \cdot \bar{\mathbf{v}}) \\
&\quad + \Delta t_k \sum_{K \in \mathcal{T}^h} (\tau_K \nabla \cdot \bar{\mathbf{u}}_k, \nabla \cdot \bar{\mathbf{v}}) \\
&= (\mathbf{u}_{k-1}, \bar{\mathbf{v}}) - 0.5\Delta t_k[(2\nu\mathbb{D}(\mathbf{u}_{k-1}), \mathbb{D}(\bar{\mathbf{v}})) + ((\mathbf{u}_{k-1} \cdot \nabla)\mathbf{u}_{k-1}, \bar{\mathbf{v}})] \\
&\quad - (\tilde{\mathbf{u}}_k^{(1)}, \bar{\mathbf{v}}) - 0.5\Delta t_k \Big[(\nu\nabla\tilde{\mathbf{u}}_k^{(1)}, \nabla\bar{\mathbf{v}}) + (((\bar{\mathbf{u}}_{k-1} + \tilde{\mathbf{u}}_k^{(1)}) \cdot \nabla)\tilde{\mathbf{u}}_k^{(1)}, \bar{\mathbf{v}}) \\
&\quad + ((\tilde{\mathbf{u}}_k^{(1)} \cdot \nabla)\bar{\mathbf{u}}_{k-1}, \bar{\mathbf{v}})\Big] + 0.5\Delta t_k(\mathbf{f}_{k-1}, \bar{\mathbf{v}}) + 0.5\Delta t_k(\mathbf{f}_k, \bar{\mathbf{v}}), \qquad (14) \\
&(\nabla \cdot \bar{\mathbf{u}}_k, \bar{q}) = 0
\end{aligned}
$$

for all $(\bar{\mathbf{v}}, \bar{q}) \in \overline{V} \times \overline{Q}$ and

$$
\begin{aligned}
&(\tilde{\mathbf{u}}_k^{(1)}, \tilde{\mathbf{v}}) + 0.5\Delta t_k \Big[((\nu + \nu_T)\nabla\tilde{\mathbf{u}}_k^{(1)}, \nabla\tilde{\mathbf{v}}) + ((\mathbf{u}_{k-1} \cdot \nabla)\tilde{\mathbf{u}}_k^{(1)}, \tilde{\mathbf{v}})\Big] \\
&= (\mathbf{u}_{k-1}, \tilde{\mathbf{v}}) - 0.5\Delta t_k[(\nu\nabla\mathbf{u}_{k-1}, \nabla\tilde{\mathbf{v}}) + ((\mathbf{u}_{k-1} \cdot \nabla)\mathbf{u}_{k-1}, \tilde{\mathbf{v}})] \\
&\quad - (\bar{\mathbf{u}}_{k-1}, \tilde{\mathbf{v}}) - 0.5\Delta t_k[(\nu\nabla\bar{\mathbf{u}}_{k-1}, \nabla\tilde{\mathbf{v}}) + ((\mathbf{u}_{k-1} \cdot \nabla)\bar{\mathbf{u}}_{k-1}, \tilde{\mathbf{v}})] \\
&\quad + \Delta t_k(\bar{p}_{k-1}, \nabla \cdot \tilde{\mathbf{v}}) + 0.5\Delta t_k(\mathbf{f}_{k-1}, \tilde{\mathbf{v}}) + 0.5\Delta t_k(\mathbf{f}_k, \tilde{\mathbf{v}}), \qquad (15)
\end{aligned}
$$

for all $\tilde{\mathbf{v}} \in \widetilde{V}^h_{\text{bub}}$.

For the steady-state bubbles, $\mathbf{u}_{k-1}$ on the right hand side of (14) is replaced by $\bar{\mathbf{u}}_{k-1}$ and the resolved small scale equation looks as follows: Find $\tilde{\mathbf{u}}_k \in \widetilde{V}^h_{\text{bub}}$ such that

$$
\begin{aligned}
&(\tilde{\mathbf{u}}_k^{(1)}, \tilde{\mathbf{v}}) + \Delta t_k \Big[((\nu + \nu_T)\nabla\tilde{\mathbf{u}}_k^{(1)}, \nabla\tilde{\mathbf{v}}) + ((\mathbf{u}_{k-1} \cdot \nabla)\tilde{\mathbf{u}}_k^{(1)}, \tilde{\mathbf{v}})\Big] \\
&= -\Delta t_k[(\nu\nabla\mathbf{u}_{k-1}, \nabla\tilde{\mathbf{v}}) + ((\bar{\mathbf{u}}_{k-1} \cdot \nabla)\bar{\mathbf{u}}_{k-1}, \tilde{\mathbf{v}}) \quad -(\bar{p}_{k-1}, \nabla \cdot \tilde{\mathbf{v}}) \\
&\quad + (\tau_K(\nabla \cdot \bar{\mathbf{u}}_{k-1}), \nabla \cdot \tilde{\mathbf{v}}) - (\mathbf{f}_k, \tilde{\mathbf{v}})], \qquad (16)
\end{aligned}
$$

for all $\tilde{\mathbf{v}} \in \widetilde{V}^h_{\text{bub}}$. Note that (16) is a decoupled system of three equations of convection–diffusion type. There is a slight difference in the resolved small scale Eq. (16) in comparison to [18,19]. The term $-\Delta t_k(\tau_K(\nabla \cdot \bar{\mathbf{u}}_{k-1}), \nabla \cdot \tilde{\mathbf{v}})$ with the model of the resolved small scale pressure is neglected in [18,19].

The crucial issue for the term $\sum_{K \in \mathcal{T}^h}(\tau_K \nabla \cdot \bar{\mathbf{u}}_k, \nabla \cdot \bar{\mathbf{v}})$ in (14), the grad–div stabilization term, consists in choosing the parameter τ_K appropriately. This stabilization term appears also in the two-scale VMS method proposed recently in [30].

2.4. Projection-based FEVMS methods based on a three-scale decomposition of the flow field

This section presents a FEVMS method which contains the projection into the large scale space explicitly as additional equation. With the help of the projection, the resolved scales are decomposed into large and small scales. Together with the unresolved scales, a three-scale decomposition of the flow field is given.

Let $V^h \times Q^h$ be a pair of inf–sup stable, conforming finite element spaces for the velocity and pressure. In addition, let L^H be a finite dimensional space of symmetric $d \times d$ tensor-valued functions representing a coarse or large scale space, and a non-negative function ν_T representing the turbulent viscosity. The semi-discrete projection-based FEVMS method seeks $\mathbf{u}^h : [0, T] \to V^h$, $p^h : (0, T] \to Q^h$, and $\mathbb{G}^H : [0, T] \to L^H$ such that

$$
\begin{aligned}
&(\mathbf{u}_t^h, \mathbf{v}^h) + (2\nu\mathbb{D}(\mathbf{u}^h), \mathbb{D}(\mathbf{v}^h)) + ((\mathbf{u}^h \cdot \nabla)\mathbf{u}^h, \mathbf{v}^h) \\
&\quad - (p^h, \nabla \cdot \mathbf{v}^h) + (\nu_T(\mathbb{D}(\mathbf{u}^h) - \mathbb{G}^H), \mathbb{D}(\mathbf{v}^h)) = (\mathbf{f}, \mathbf{v}^h) \quad \forall \mathbf{v}^h \in V^h, \\
&(q^h, \nabla \cdot \mathbf{u}^h) = 0 \quad \forall q^h \in Q^h, \\
&(\mathbb{D}(\mathbf{u}^h) - \mathbb{G}^H, \mathbb{L}^H) = 0 \quad \forall \mathbb{L}^H \in L^H. \qquad (17)
\end{aligned}
$$

The tensor $\mathbb{G}^H$ represents the large scales of $\mathbb{D}(\mathbf{u}^h)$. These scales are defined by the L^2-projection of $\mathbb{D}(\mathbf{u}^h)$ into the large scale space L^H, the third equation in (17). The difference $\mathbb{D}(\mathbf{u}^h) - \mathbb{G}^H$ represents the resolved small scales. Besides this additional projection, the projection-based FEVMS method introduces a viscous term into the momentum equation, the last term on the left hand side. It can be seen clearly in this term that the turbulent viscosity ν_T acts directly only on the resolved small scales.

Besides the explicit appearance of the projection operator, there is another principal difference between the projection-based approach and the bubble-based FEVMS method. In the latter, the large scales are given in standard finite element spaces and one needs an additional higher resolution finite element space for the resolved small scales. In contrast, in the projection-based FEVMS method, all resolved scales belong to standard finite element spaces and an additional large scale space is needed. Since all resolved scales are contained in the standard finite element spaces, whose functions are not restricted to single mesh cells, the projection-based FEVMS method does not introduce scales which cannot move freely.

The projection terms in (17) can be treated explicitly or implicitly in time, see [27]. We will restrict here to the implicit treatment, see the end of this section for comments on the explicit approach. The fully implicit projection-based FEVMS method, discretized by the Crank–Nicolson scheme, has the form: Find $(\mathbf{u}_k^h, p_k^h) \in V^h \times Q^h$ such that

$$
\begin{aligned}
&(\mathbf{u}_k^h, \mathbf{v}^h) + 0.5\Delta t_k \Big[(2Re^{-1}\mathbb{D}(\mathbf{u}_k^h), \mathbb{D}(\mathbf{v}^h)) + ((\mathbf{u}_k^h \cdot \nabla)\mathbf{u}_k^h, \mathbf{v}^h) \\
&\quad + \big(\nu_{T,k}(\mathbb{D}(\mathbf{u}_k^h) - \mathbb{G}_k^H), \mathbb{D}(\mathbf{v}^h)\big)\Big] - (p_k, \nabla \cdot \mathbf{v}^h) \\
&= (\mathbf{u}_{k-1}^h, \mathbf{v}^h) - 0.5\Delta t_k \Big[(2Re^{-1}\mathbb{D}(\mathbf{u}_{k-1}^h), \mathbb{D}(\mathbf{v}^h)) \\
&\quad + ((\mathbf{u}_{k-1}^h \cdot \nabla)\mathbf{u}_{k-1}^h, \mathbf{v}^h) \qquad (18) \\
&\quad + \big(\nu_{T,k-1}(\mathbb{D}(\mathbf{u}_{k-1}^h) - \mathbb{G}_{k-1}^H), \mathbb{D}(\mathbf{v}^h)\big)\Big] \\
&\quad + 0.5\Delta t_k(\mathbf{f}_{k-1}, \mathbf{v}^h) + 0.5\Delta t_k(\mathbf{f}_k, \mathbf{v}^h) \quad \forall \mathbf{v}^h \in V^h, \\
&(q^h, \nabla \cdot \mathbf{u}_k^h) = 0 \quad \forall q^h \in Q^h, \\
&\big(\mathbb{G}_k^H - \mathbb{D}(\mathbf{u}_k^h), \mathbb{L}^H\big) = 0 \quad \forall \mathbb{L}^H \in L^H.
\end{aligned}
$$

The efficient implementation of this method was studied in [12]. The main features of the fully implicit approach are:

- it is only efficient if L^H is a discontinuous finite element space on the finest grid and the basis of L^H is chosen to be L^2-orthogonal,
- seven sparse matrices whose dimensions depend on V^h and L^H are needed,
- four of these matrices have to be assembled only once at the initial time,
- the three other matrices have to be assembled at each discrete time in each step of the iteration for solving the nonlinearity, since they depend on ν_T and ν_T depends on the current finite element solution,
- sparse matrix–matrix products have to be computed at each discrete time in each step of the iteration for solving the nonlinearity.

For the turbulent viscosity, eddy viscosity models of Smagorinsky-type will be used

$$\nu_T = C_S\delta^2\|\mathbb{D}(\mathbf{u}^h)\|_F, \tag{19}$$

$$\nu_T = C_S\delta^2\|\mathbb{D}(\mathbf{u}^h) - \mathbb{G}^H\|_F. \tag{20}$$

The model (19) uses all resolved scales in the turbulent viscosity whereas (20) uses only the resolved small scales.

Remark. In [27], the differences between the explicit and implicit treatment of the projection terms, i.e. the additional viscous term and the additional equation in (17), were studied. Using the eddy viscosity model (19), the results obtained with both approaches were very similar. The explicit approach saved 5–10% of computing time. For the resolved small scale eddy viscosity (20), the results obtained with both approaches were quite different. In particular, rather bad results were obtained with the explicit approach. Since the resolved small scales show strong fluctuations, it makes a difference whether in (20) the resolved small scales from the present or the previous discrete time were used.

3. Numerical studies

We studied the different types of FEVMS methods at the benchmark problems of the turbulent channel flows at $Re_\tau = 180$ and $Re_\tau = 395$. The setup of the problems and the reference values have been taken from [45].

3.1. The setup of the numerical studies

The turbulent channel flow at $Re_\tau = 180$ is given in $\Omega = (-2\pi, 2\pi) \times (0, 2) \times (-2\pi/3, 2\pi/3)$. The domain of the turbulent channel flow at $Re_\tau = 395$ is $\Omega = (-\pi, \pi) \times (0, 2) \times (-\pi/2, \pi/2)$. The parameter in the Navier–Stokes equations (1) is set to be $\nu = 1/180$ or $\nu = 1/395$, respectively. No-slip boundary conditions are described at $y = 0$ and $y = 2$. On all other boundaries, periodic conditions are applied.

The flows are driven by a pressure gradient in x-direction, i.e. the right hand side of the Navier–Stokes equations has the form $\mathbf{f} = (f_1, 0, 0)^T$. In our computations, the value of f_1 was adjusted dynamically (around the value 1) such that the bulk velocity of the flow is kept close to a prescribed value, $U_{\text{bulk}} = 15.6803$ for $Re_\tau = 180$ and $U_{\text{bulk}} = 17.5452$ for $Re_\tau = 395$. These values have been computed using the reference mean velocities from [45]. The dynamic adjustment of the right hand side was found to be necessary in [26] because the velocity finite element functions are only discretely divergence-free. Thus, the finite element methods preserve mass only approximately. Without a dynamic adjustment of the right hand side, considerable losses or gains of mass could be observed in long time computations. Note that this unfavorable property of finite element methods is of high importance in the turbulent channel flow examples because of the non-physical periodic boundary conditions. These boundary conditions model an infinitely long channel. In applications, the flow domain is generally finite and the approximate conservation of mass will effect the computational results much less. For details on the dynamic adjustment procedure, we refer to [26].

The Navier–Stokes equations (1) have been discretized in time by the Crank–Nicolson scheme with an equidistant time step of $\Delta t = 0.004$ for $Re_\tau = 180$ and $\Delta t = 0.002$ for $Re_\tau = 395$. Let $\Delta t^+ := u_\tau Re_\tau \Delta t$. This gives, for the statistically steady state $u_\tau = 1$, $\Delta t^+ = 0.72$ for $Re_\tau = 180$ and $\Delta t^+ = 0.79$ for $Re_\tau = 395$. These time steps are smaller than the Kolmogorov time scale and they are in the range proposed in [46].

The computations were performed in three stages. In the first stage, we started with an initial condition where the mean velocity field from [45] for a given Reynolds number was superimposed with random noise, see [26] for details. The computations used a projection-based FEVMS method and they were performed 20 s (seconds). ($t^+ \in [0, 3600]$ for $Re_\tau = 180$, $t^+ \in [0, 7900]$ for $Re_\tau = 395$). The resulting flow field was used as initial condition for all simulations of the second stage. In the second stage, the flow field was allowed another 10 s. to develop with the considered FEVMS method. Afterwards, in the third stage, the statistics were computed over a period of 20 s.

The velocity was discretized with the Q_2 finite element and the pressure with the discontinuous P_1^{disc} finite element on hexahedral grids. This pair of inf–sup stable finite element spaces is among the best performing ones for the incompressible Navier–Stokes equations [47,36,34]. The grids were uniformly refined in streamwise and spanwise direction. In wall-normal direction, they became finer towards the walls. We will present results for a grid for which the positions of the grid points in wall-normal direction are given by

$$y_i = 1 - \cos\left(\frac{i\pi}{N_y}\right), \quad i = 0, \ldots, N_y.$$

Here, N_y is the number of mesh cell layers in wall-normal direction. We also performed simulations with different grids (Grids 2 and 3 from [27]), which led to the same qualitative results and conclusions as given below. The grids originate from the refinement of coarse grids (Level 0), see Table 1 for information on the grids. Level 2 is sufficiently coarse such that simulations with the Galerkin finite element discretization blow up in finite times. In the case $Re_\tau = 395$, the Galerkin finite element method blows up in finite time also on Level 3. In all situations studied in this paper, the use of a turbulence model is necessary to perform any simulations at all.

The important parameter in the bubble-based FEVMS method with grad–div stabilization (14) and (16) is τ_K, which is introduced from the model (13) for the resolved small scale pressure. In the turbulent channel flows presented below, inf–sup stable finite elements on anisotropic grids are used. For this combination, an appropriate choice of τ_K is not yet known. We tested a choice which is advised for inf–sup stable finite elements on isotropic meshes, [22],

$$\tau_K = C = \frac{1}{2}, \tag{21}$$

and a choice similar to that which was used for equal-order finite element spaces in [18,19] and which was originally proposed in [48]

$$\tau_K = \frac{1}{2}\sqrt{\nu^2 + \left(\frac{C_2 h_K \|\mathbf{u}^h\|_2}{C_1}\right)^2} \tag{22}$$

with the constants $C_1 = 2$, $C_2 = 1$ and h_K twice the minimal length of an edge of the mesh cell K. In the recently proposed two-scale VMS method [30], another choice for τ_K was proposed which also takes the length of the time step into account. For hexahedral mesh cells, the formula from [30] shows similarities to (22) if the term containing the length of the time step is neglected.

The local systems in the bubble-based FEVMS methods for approximating the solution of (11), (12), (15) and (16) were solved on grids with $3 \times 3 \times 3$ or $5 \times 5 \times 5$ small mesh cells, similar to [18,19] where for instance $4 \times 4 \times 4$ mesh cells were used. For (11) and (12), the Q_2/Q_1 pair of finite elements was used and for

Table 1
Information on the spatial discretizations used in the simulations.

Level	Cells	N_y	Vel. d.o.f.	Press. d.o.f.	y^+_{min}
2	1024	16	25,344	4096	1.7293
3	8112	32	199,680	32,768	0.4386

(15) and (16) the Q_1 finite element discretization. There is a difficulty in the application of the bubble method to the Q_2 finite element since this finite element has one basis function which is a bubble function, such that there is no direct sum decomposition of the spaces. In this case, one should project the right hand side of (11) and (12) into an appropriate subspace. We could not however find in the literature any hints on how to implement a bubble finite element method for higher order finite elements, not even for scalar equations. Since the bubble Eqs. (11) and (12) are for the bubble-based FEVMS methods only an auxiliary problem, the issue of the projection was just neglected. We do not think that the blow-up in finite time of the bubble-based FEVMS method (10), (11) and (10), (12) could be prevented with the application of a projection in the bubble equations since the instability of this approach arises in our opinion from the Galerkin finite element matrix in the large scale equation.

The following eddy viscosity models were used for the bubble-based FEVMS methods:

- the all-small Smagorinsky model (9) with $\mathbf{u}_{k-1}$ and $C_S = 1$ for the methods (10), (11) and (14), (15) with time-dependent resolved small scales,
- the large-small Smagorinsky model (8) with $\bar{\mathbf{u}}_{k-1}$ and $C_S \in \{0.5, 1\}$ for the methods (10), (12) and (14), (16) with steady resolved small scales.

For more standard values of the constant, like $C_S \in \{0.01, 0.1\}$, the coupled systems of equations blew up in finite time. We think that a reason for the need of large constants C_S is the use of very coarse grids for the resolved small scales. The local problems to be solved on these grids are similarly convection-dominated like the global problem and a lot of additional viscosity is necessary in order to stabilize them. For the projection-based FEVMS method (18), both variants (19) and (20) of the eddy viscosity model were tested. The parameter δ was chosen to be twice the smallest length of an edge of the mesh cells. This is the same choice as in [26,27].

In our opinion, a potential advantage of many VMS methods is that simple models for the influence of the unresolved scales can be applied since these models act directly only on a part of the resolved scales and the importance of the model is reduced in this way. The use of the constant Smagorinsky model is common in VMS methods [6,7,13–15,49]. Several studies found that the application of the dynamic Smagorinsky model in VMS methods does not improve the results compared with the constant Smagorinsky model, [13,49,15], sometimes the results were even worse with the dynamic model [13,49]. In view of these experiences, the application of the dynamic Smagorinsky model does not seem to be essential for studying the potential of VMS methods.

The following abbreviations are used below:

- RFBn_td – residual-free bubble-based FEVMS method (14) and (15) with time-dependent resolved small scales, grad–div stabilization and with $n \times n \times n$ meshes for approximating the local solutions,
- RFBn_red – reduced residual-free bubble-based FEVMS method (14) and (16) with grad–div stabilization and with $n \times n \times n$ meshes for approximating the local solutions,
- tau_c – constant τ_K defined in (21),
- tau_nc – non-constant τ_K defined in (22),
- VMSn – projection-based VMS with $L^H = P_0$ if $n = 0$ and $L^H = P_1^{\text{disc}}$ if $n = 1$,
- ALL – all-small model (19),
- SMALL – small–small model (20).

The values of interest which have been studied are (the difference to) the mean velocity profile, the rms turbulence intensity $u^{h,*}_{\text{rms}}$, and the off-diagonal Reynolds stress component $\mathbb{R}^{h,*}_{12}$. For the definition of these quantities and their computation, see [26]. The simulations were performed with the code MooNMD [50].

3.2. Simulations for the turbulent channel flow at $Re_\tau = 180$

Numerical studies for turbulent channel flows at $Re_\tau = 180$ with projection-based FEVMS methods can be found in [26,27]. An observation in [26] was that the fully implicit projection-based FEVMS method gave better results than the traditional Smagorinsky LES with van Driest damping. For this reason, we do not include any comparison with the latter method into the present paper. Another observation in [26,27] was that (the absolute values of) second order statistics were overpredicted. We are not aware of any turbulent channel flow computations with bubble-based FEVMS methods. All computations for $Re_\tau = 180$ presented in this section were performed on Level 2.

The computations with the bubble-based FEVMS methods (10), (11) and (10), (12) with time-dependent resolved small scales blew up after around 0.2–0.25 s. Removing the influence of the resolved small scales onto the large scales, we found that for the all-small Smagorinsky model with $C_S = 1$ the blow-up of the simulations is not caused directly by a blow-up of the simulations of the equations for the resolved small scales because then the simulations blew up considerably later. The reason of the blow-up is in our opinion that the matrix of the equations for the large scales is the same matrix as in the Galerkin finite element method. In addition, the blow-ups suggest that in these simulations the use of the pressure bubbles is not equivalent to the inclusion of a grad–div stabilization term as for the Stokes equations. This might have several reasons, for instance the dominating convection in turbulent flows or the use of anisotropic mesh cells in turbulent channel flow simulations.

Fig. 1 shows results obtained with the reduced bubble-based FEVMS with grad–div term and with time-dependent and steady resolved small scales (14), (15) and (14), (16). It can be seen that the use of time-dependent resolved small scales leads to some oscillations in the mean velocity profile and to an overprediction of U^h_{mean} near the walls. In comparison with other schemes, the use of time-dependent resolved small scales seems to introduce less viscosity. Another hint in this direction is that it was much harder to solve the equations for the large scales with this approach. Considering the computational costs and the obtained results, we think that the use of time-dependent resolved small scales in the way studied in this paper does not pay off.

The results with the reduced bubble-based FEVMS method (14) and (16) were often improved by solving the local problems on $5 \times 5 \times 5$ meshes in comparison with $3 \times 3 \times 3$ meshes, see Fig. 2. Only $u^{h,*}_{\text{rms}}$ is oscillatory in the center of the channel for RFB5. The computational costs for local $3 \times 3 \times 3$ meshes were less than the costs of one multigrid cycle for the large scale equations whereas the costs of using $5 \times 5 \times 5$ meshes were about the costs of four multigrid cycles. Since different resolved small scales were obtained in both cases, their effect in the large scale equations is different and the solver of these equations behaves differently. In fact, we could observe that the solver often needed fewer iterations if the resolved small scales were computed on the finer local mesh. Thus, the total computing times of both approaches were in general comparable.

Fig. 3 compares results obtained with the reduced bubble-based FEVMS methods with grad–div stabilization (14) and (16) for different values of C_S. In addition, in order to see the influence of the resolved small scale terms in the large scale Eq. (14), results for simulations which neglect these terms are included, i.e. the grad–div stabilization is the only model (nobubble). It can be seen that this simple approach led, in comparison with some of the

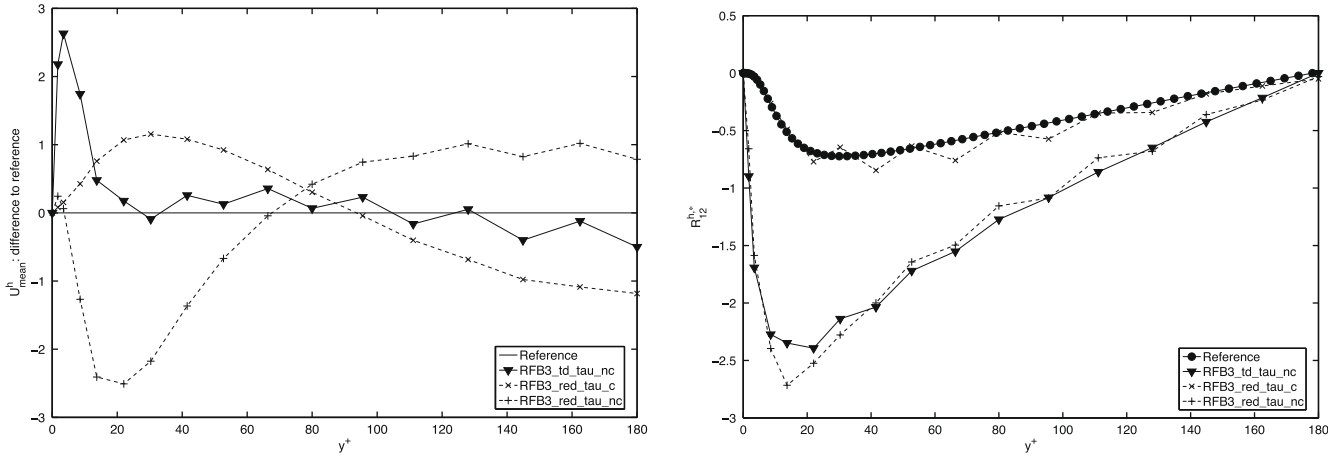

Fig. 1. Turbulent channel flow at $Re_\tau = 180$, bubble-based FEVMS methods with grad–div stabilization, time-dependent and steady resolved small scales, $C_S = 1$ in (9) and (8).

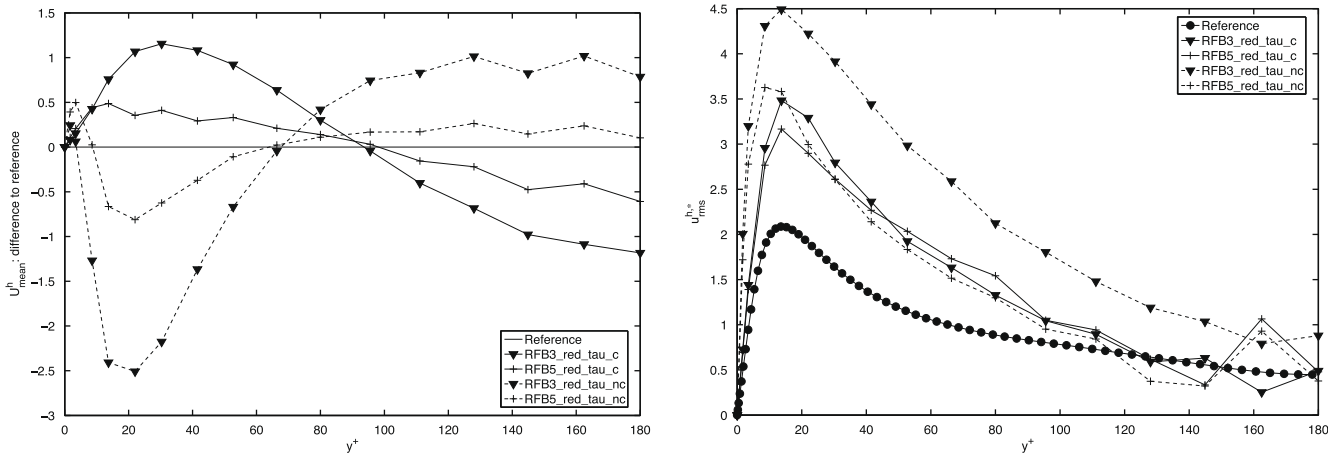

Fig. 2. Turbulent channel flow at $Re_\tau = 180$, reduced bubble-based FEVMS method with grad–div stabilization, different sizes of the local grids, $C_S = 1$ in (8).

other approaches, to reasonable results. Using also the resolved small scale terms, in addition to the grad–div term, improves in general the results. But there is no combination of the parameters τ_K and C_S which proved to be best in all respects.

In our opinion, the definition (22) of τ_K gave often slightly better results than (21). One computation which used (22), $5 \times 5 \times 5$ local grids and $C_S = 1$ is compared with projection-based FEVMS methods in Fig. 4. It can be seen that this method RFB5 gives the

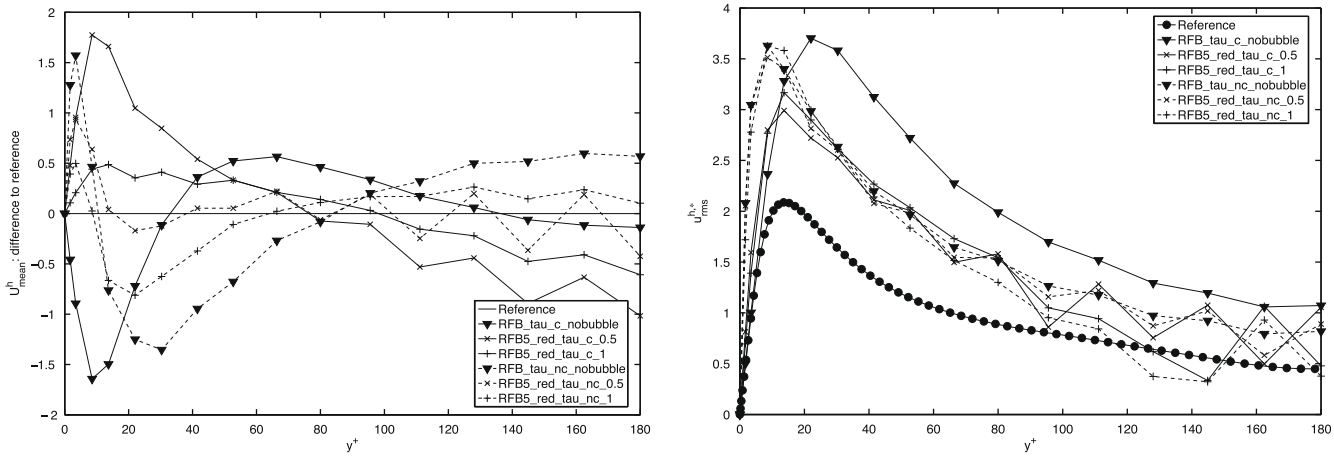

Fig. 3. Turbulent channel flow at $Re_\tau = 180$, reduced bubble-based FEVMS method with grad–div stabilization, Smagorinsky model (8) with different values of C_S.

best results for $u^{h,*}_{\mathrm{rms}}$, apart from the center of the channel. With respect to $\mathbb{R}^{h,*}_{12}$, the method VMS0 gives the best results near the walls and RFB5 in the center of the channel. RFB5 and VMS1 give similar mean velocity profiles. Altogether, the best bubble-based FEVMS method leads to slightly better results than the projection-based FEVMS methods.

3.3. Simulations for the turbulent channel flow at $Re_\tau = 395$

Neither for the bubble-based FEVMS methods nor for the projection-based FEVMS methods simulations for this example can be found in the literature so far. Here, results computed on Level 2 and on Level 3 will be presented. We could observe that for the projection-based FEVMS methods the results for $C_S = 0.01$ in (19) and (20) were in general better than for $C_S = 0.005$. This agrees with the observations for $Re_\tau = 180$ in [26,27]. For brevity, only the results for $C_S = 0.01$ will be presented. For the bubble-based FEVMS method (14) and (16), we present results for $C_S = 1$. With $C_S = 0.5$, often rather bad results were obtained.

The second order statistics were often considerably overpredicted on Level 2, see Fig. 5 These statistics measure in some sense the turbulent character of the simulated flow. Obviously, the FEVMS methods do not introduce sufficient viscosity on these coarse grids. The less viscosity is introduced, the larger the overpredictions are, for instance, the overpredictions are larger for VMS1 than for VMS0. The results of VMS0 and RFB5_red_tau_nc are often comparable. Only concerning the mean velocity profile, the bubble-based FEVMS methods gave better results near the wall and VMS0 in the center of the channel.

Considering only the projection-based FEVMS methods, one can observe that the results obtained with VMS0 are better than those computed with VMS1. There are only slight differences between both variants (19) and (20) of the Smagorinsky model. In general, the curves obtained with using all scales (19) are somewhat closer to the reference curves. The results show that the definition of the large scale space L^H is more important than the actual form of the Smagorinsky model.

It can be seen in Fig. 6 that the differences to all reference curves are much smaller on Level 3 than on Level 2. The bubble-based FEVMS method RFB5_red_tau_nc is closest to the reference curves for U^h_{mean} and $\mathbb{R}^{h,*}_{12}$ whereas the projection-based FEVMS methods approximate $u^{h,*}_{\mathrm{rms}}$ in the center of the channel somewhat better.

Remark. Concerning the computational costs, we could observe that in general:

- simulations with VMS0 were somewhat faster than with VMS1,
- computations of the projection-based methods with (19) were a little faster than with (20),
- bubble-based FEVMS methods with grad–div stabilization were considerably faster with $C_S = 1$ in (8) than with $C_S = 0.5$,
- bubble-based FEVMS methods with grad–div stabilization and $C_S = 1$ were faster than VMS0, bubble-based FEVMS methods with $C_S = 0.5$ were somewhat slower than VMS0.

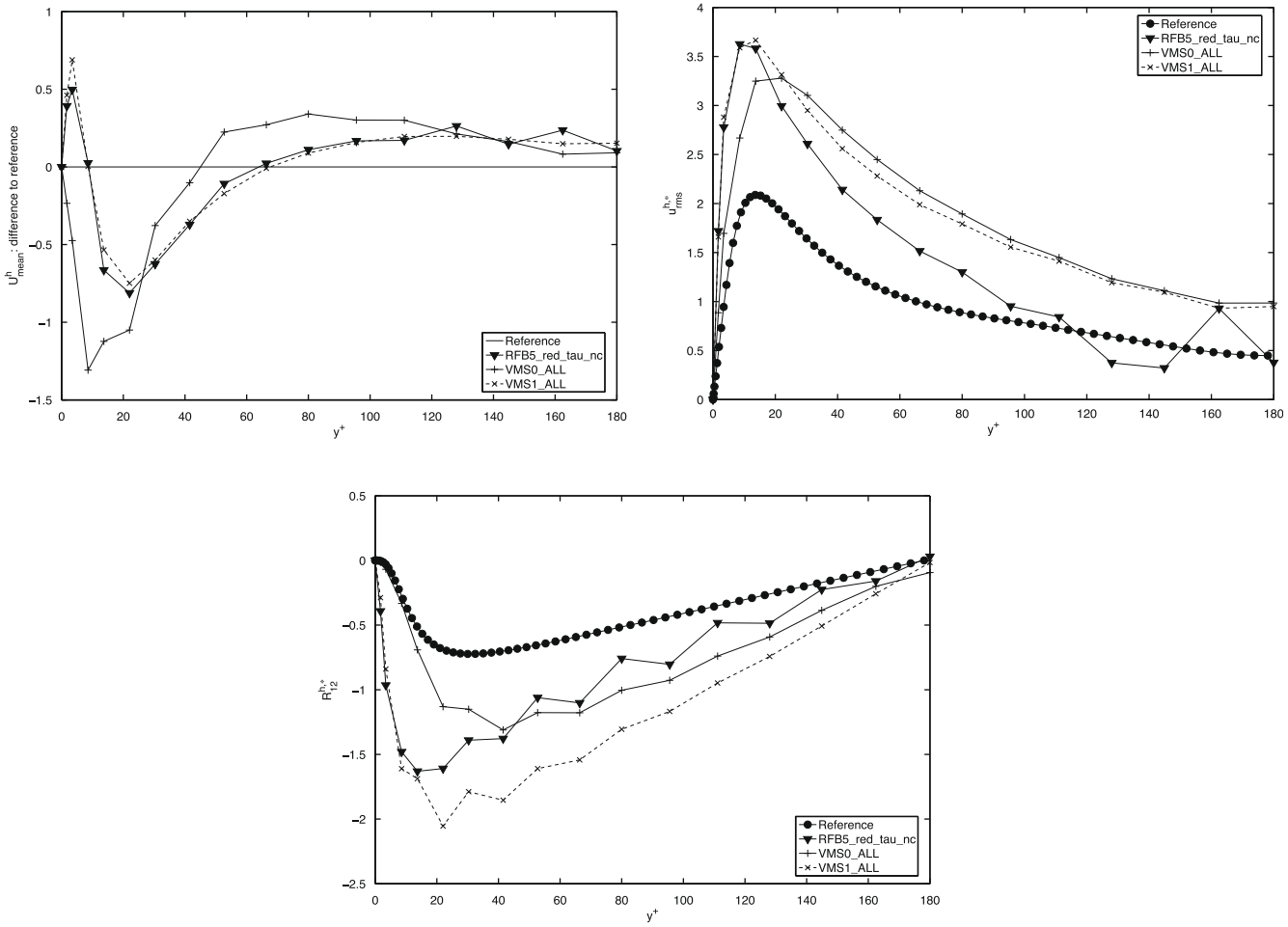

Fig. 4. Turbulent channel flow at $Re_\tau = 180$, comparison of the FEVMS methods.

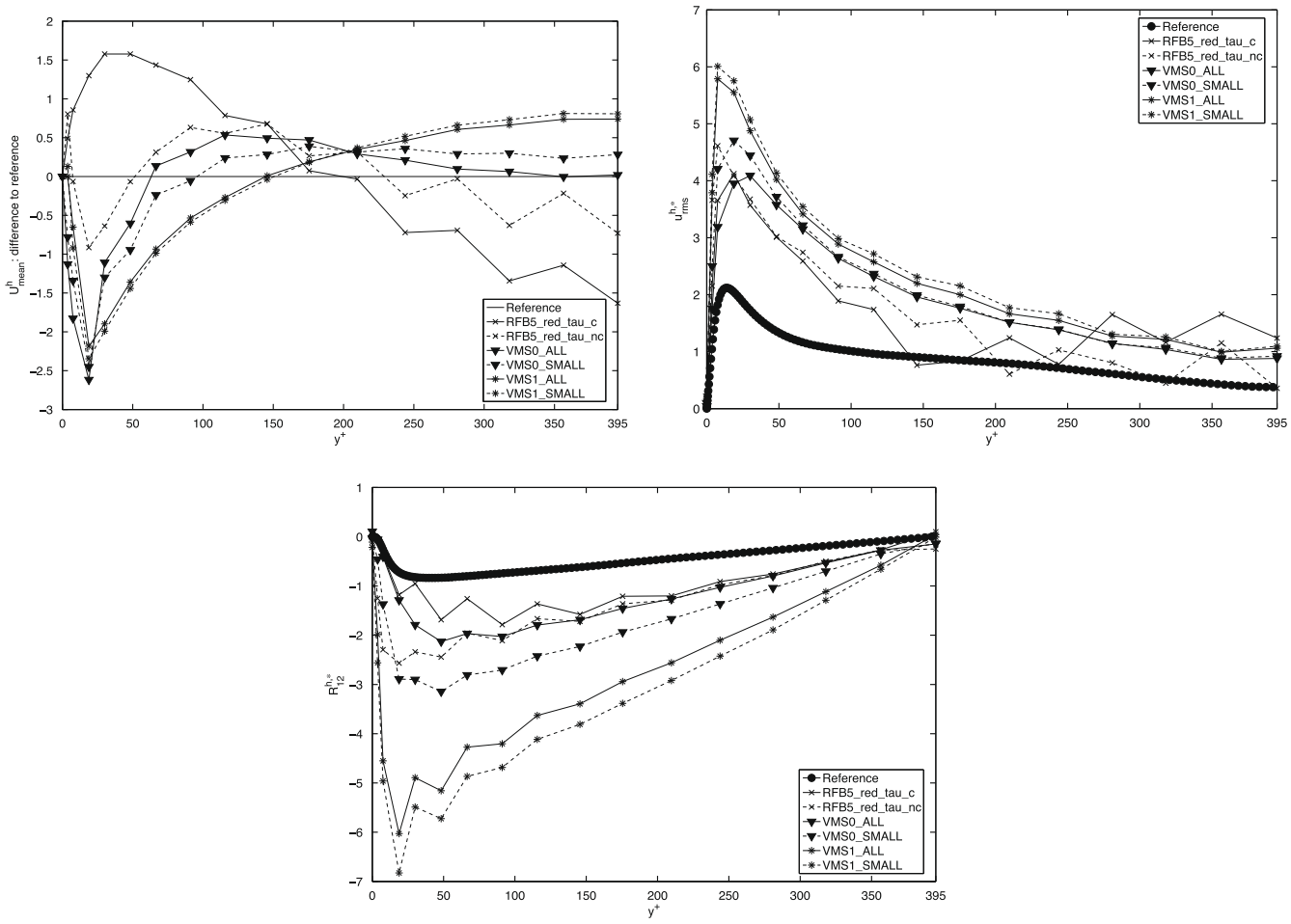

Fig. 5. Turbulent channel flow at $Re_\tau = 395$, Level 2, comparison of the FEVMS methods.

3.4. Discussion of the results

All FEVMS methods showed in general an overprediction of (the absolute values) of the second order statistics. Based on results from the literature and on our own experiences, there are two reasons in our opinion. Compared with spectral methods, which are often used in turbulent channel flow simulations, a rather low-order spatial discretization (second order) was used. One can find large overpredictions of second order statistics also in other simulations with second order spatial discretizations, [13,51]. Our motivation for using finite element methods is that they can be also used in more complicated domains, which will be the general case in applications. The second reason for the large overprediction of the second order statistics are the coarse meshes, see the introduction for the motivation of using them. Moreover, it was seen in Section 3.3 that the overpredictions became considerably smaller if the meshes are refined.

The numerical studies of the bubble-based FEVMS methods show that the very coarse meshes which are used for solving the local problems led to difficulties. Since the local problems are similarly convection-dominated as the global problem, it turned out that a lot of viscosity had to be introduced in order to stabilize the local systems, i.e. the Smagorinsky constant had to be chosen rather large. It was demonstrated that the choice of this constant has a considerable influence on the solutions. In this respect, also the question arises how useful are the computed resolved small scales if the equations are dominated by the viscosity model on the affordable coarse local grids. It is remarkable that removing the resolved small scale terms from the large scale equation and using only the grad–div stabilization gave still reasonable results. The grad–div term seems to us to be the more important model, which is also supported by the blow-up of the bubble-based FEVMS without grad–div term. We think that it is more promising to eliminate the use of bubble functions and to study the two-scale VMS method from [30], which also contains a grad–div stabilization term. This approach would also eliminate the computational overhead of assembling and solving the local problems as well as the unphysical modeling of the resolved small scales as described at the end of Section 2.2.

Among the projection-based FEVMS methods, the method which introduced the most viscosity gave the best results, namely VMS0 with all resolved scales in the Smagorinsky model (19). It could be observed that the large scale space L^H had a much higher impact on the results than the eddy viscosity model, i.e. (19) or (20).

Often, the best reduced bubble-based FEVMS and VMS0 gave comparable results in comparable computing times.

4. Summary and outlook

Two principal different approaches of FEVMS methods were applied at turbulent channel flow simulations on rather coarse grids. Several variants for both approaches were assessed, details of the assessment can be found in Section 3.4.

A main conclusion of the numerical studies is that the application of bubble-based FEVMS methods is quite complicated. It has to

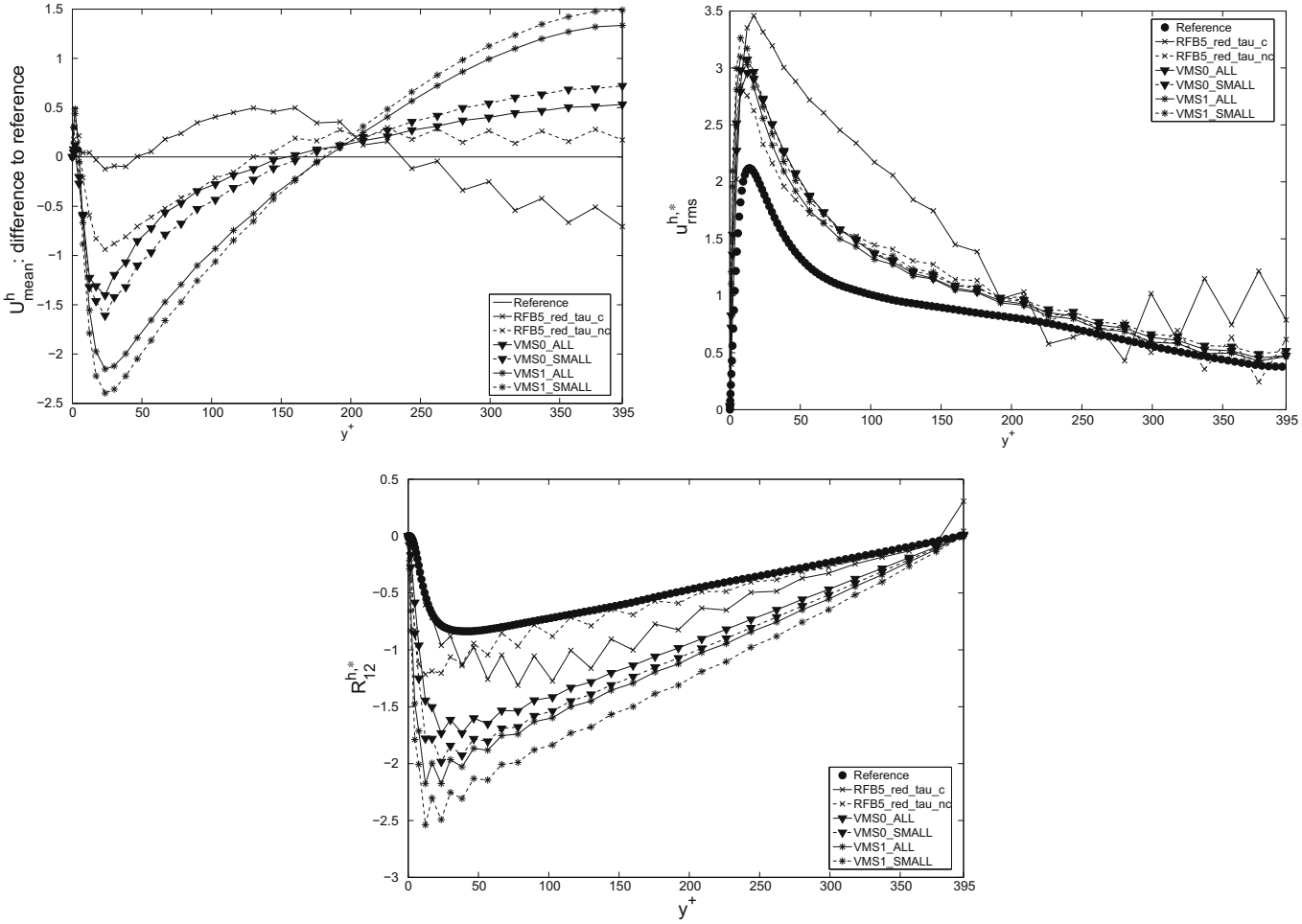

Fig. 6. Turbulent channel flow at $Re_\tau = 395$, Level 3, comparison of the FEVMS methods.

be decided which simplifying assumptions for the resolved small scales are permissible, how fine should the local meshes be and which models for ν_T and τ_K should be used. The numerical studies showed that the grad–div term, as model for the resolved small scale pressure, possesses a high importance. In addition, the usefulness of the computed resolved small scales is questionable because of the dominating influence of the viscosity model in the numerical solution of these equations on very coarse local grids. In view of our experiences, we think that it is more promising, and also easier from the computational point of view, to consider the recently proposed two-scale VMS method from [30] which contains several stabilization terms, among them a grad–div term.

The numerical results for the projection-based FEVMS methods showed that the choice of the large scale space has the essential influence on the results. The next step in our research will be the design of an adaptive projection-based FEVMS where the large scale space is chosen differently on different mesh cells and where this choice is done a posteriori, i.e. during the simulations.

References

[1] B. Mohammadi, O. Pironneau, Analysis of the K-Epsilon Turbulence Model, John Wiley & Sons, 1994.
[2] P. Sagaut, Large Eddy Simulation for Incompressible Flows, 3rd ed., Springer-Verlag, Berlin, Heidelberg, New York, 2006.
[3] T. Hughes, Multiscale phenomena: Green's functions, the Dirichlet-to-Neumann formulation, subgrid-scale models, bubbles and the origin of stabilized methods, Comput. Methods Appl. Mech. Engrg. 127 (1995) 387–401.
[4] J.-L. Guermond, Stabilization of Galerkin approximations of transport equations by subgrid modeling, M2AN 33 (1999) 1293–1316.
[5] T. Hughes, L. Mazzei, K. Jansen, Large Eddy simulation and the variational multiscale method, Comput. Visual. Sci. 3 (2000) 47–59.
[6] T. Hughes, L. Mazzei, A. Oberai, A. Wray, The multiscale formulation of large Eddy simulation: decay of homogeneous isotropic turbulence, Phys. Fluids 13 (2001) 505–512.
[7] T. Hughes, A. Oberai, L. Mazzei, Large Eddy simulation of turbulent channel flows by the variational multiscale method, Phys. Fluids 13 (2001) 1784–1799.
[8] V. John, Large Eddy simulation of turbulent incompressible flows. Analytical and Numerical Results for a Class of LES Models, Lecture Notes in Computational Science and Engineering, vol. 34, Springer-Verlag, Berlin, Heidelberg, New York, 2004.
[9] A. Dunca, V. John, W. Layton, The commutation error of the space averaged Navier–Stokes equations on a bounded domain, in: J.H.G.P. Galdi, R. Rannacher (Eds.), Contributions to Current Challenges in Mathematical Fluid Mechanics, Birkhäuser, 2004, pp. 53–78.
[10] L. Berselli, V. John, Asymptotic behavior of commutation errors and the divergence of the reynolds stress tensor near the wall in the turbulent channel flow, Math. Methods Appl. Sci. 29 (2006) 1709–1719.
[11] L. Berselli, C. Grisanti, V. John, Analysis of commutation errors for functions with low regularity, J. Comput. Appl. Math. 206 (2007) 1027–1045.
[12] V. John, S. Kaya, A finite element variational multiscale method for the Navier–Stokes equations, SIAM J. Sci. Comput. 26 (2005) 1485–1503.
[13] V. Gravemeier, Scale-separating operators for variational multiscale large Eddy simulation of turbulent flows, J. Comput. Phys. 212 (2006) 400–435.
[14] J. Holmen, T. Hughes, A. Oberai, G. Wells, Sensitivity of the scale partition for variational multiscale large-Eddy simulation of channel flow, Phys. Fluids 16 (2004) 824–827.
[15] C. Farhat, A. Rajasekharan, B. Koobus, A dynamic variational multiscale method for large Eddy simulations on unstructured meshes, Comput. Methods Appl. Mech. Engrg. 195 (2006) 1667–1691.
[16] V. Gravemeier, The variational multiscale method for laminar and turbulent flow, Arch. Comput. Methods Engrg. 13 (2006) 249–324.
[17] V. Gravemeier, The Variational Multiscale Method for Laminar and Turbulent Incompressible Flow. Ph.D. Thesis, Institute of Structural Mechanics, University of Stuttgart, 2003.

[18] V. Gravemeier, W. Wall, E. Ramm, A three-level finite element method for the instationary incompressible Navier–Stokes equation, Comput. Methods Appl. Mech. Engrg. 193 (2004) 1323–1366.
[19] V. Gravemeier, W. Wall, E. Ramm, Large Eddy simulation of turbulent incompressible flows by a three-level finite element method, Int. J. Numer. Methods Fluids 48 (2005) 1067–1099.
[20] L. Franca, S. Oliveira, Pressure bubbles stabilization features in the Stokes problem, Comput. Methods Appl. Mech. Engrg. 192 (2003) 1929–1937.
[21] L. Franca, S. Frey, Stabilized finite element methods: II. The incompressible Navier–Stokes equations, Comput. Methods Appl. Mech. Engrg. 99 (1992) 209–233.
[22] M. Braack, E. Burman, V. John, G. Lube, Stabilized finite element methods for the generalized oseen problem, Comput. Methods Appl. Mech. Engrg. 196 (2007) 853–866.
[23] S. Collis, Monitoring unresolved scales in multiscale turbulence modeling, Phys. Fluids 13 (2001) 1800–1806.
[24] K. Jansen, A. Tejada-Martinez, An Evaluation of the Variational Multiscale Model for Large-Eddy Simulation While Using a Hierarchical Basis, AIAA Paper 2002–0283.
[25] S. Ramakrishnan, S. Collis, Multiscale Modeling for Turbulence Simulation in Complex Geometries, AIAA Paper, 2004.
[26] V. John, M. Roland, Simulations of the turbulent channel flow at $Re_\tau = 180$ with projection-based finite element variational multiscale methods, Int. J. Numer. Methods Fluids 55 (2007) 407–429.
[27] V. John, A. Kindl, Variants of projection-based finite element variational multiscale methods for the simulation of turbulent flows, Int. J. Numer. Methods Fluids 56 (2008) 1321–1328.
[28] M. Germano, U. Piomelli, P. Moin, W. Cabot, A dynamic subgrid-scale Eddy viscosity model, Phys. Fluids A 3 (1991) 1760–1765.
[29] D. Lilly, A proposed modification of the Germano subgrid-scale closure method, Phys. Fluids A 4 (1992) 633–635.
[30] Y. Bazilevs, V. Calo, J. Cottrell, T. Hughes, A. Reali, G. Scovazzi, Variational multiscale residual-based turbulence modeling for large Eddy simulation of incompressible flows, Comput. Methods Appl. Mech. Engrg. 197 (2007) 173–201.
[31] T. Hughes, G. Sangalli, Variational multiscale analysis: the fine-scale Green's function, projection, optimization, localization, and stabilized methods, SIAM J. Numer. Anal. 45 (2007) 539–557.
[32] J.-M. Senoner, M. Garcia, S. Mendez, G. Staffelbach, O. Vermorel, T. Poinsot, The growth of rounding errors and the repetitivity of large Eddy simulation, AIAA J. 46 (2008) 1773–1781.
[33] R. Adams, Sobolev Spaces, Academic Press, New York, 1975.
[34] V. John, Reference values for drag and lift of a two-dimensional time dependent flow around a cylinder, Int. J. Numer. Methods Fluids 44 (2004) 777–788.
[35] V. John, G. Matthies, J. Rang, A comparison of time-discretization/linearization approaches for the time-dependent incompressible Navier–Stokes equations, Comput. Methods Appl. Mech. Engrg. 195 (2006) 5995–6010.
[36] V. John, Higher order finite element methods and multigrid solvers in a benchmark problem for the 3D Navier–Stokes equations, Int. J. Num. Methods Fluids 40 (2002) 775–798.
[37] V. John, On the efficiency of linearization schemes and coupled multigrid methods in the simulation of a 3D flow around a cylinder, Int. J. Numer. Methods Fluids 50 (2006) 845–862.
[38] F. Brezzi, L. Franca, T. Hughes, A. Russo, $b = \int g$, Comput. Methods Appl. Mech. Engrg. 145 (1997) 329–339.
[39] V. John, On large Eddy simulation and variational multiscale methods in the numerical simulation of turbulent incompressible flows, Appl. Math. 51 (2006) 321–353.
[40] J. Smagorinsky, General circulation experiments with the primitive equations, Mon. Weather Rev. 91 (1963) 99–164.
[41] A. Russo, Bubble stabilization of finite element methods for the linearized incompressible Navier–Stokes equations, Comput. Methods Appl. Mech. Engrg. 132 (1996) 335–343.
[42] R. Codina, J. Principe, O. Guasch, S. Badia, Time dependent subscales in the stabilized finite element approximation of incompressible flow problems, Comput. Methods Appl. Mech. Engrg. 196 (2007) 2413–2430.
[43] L. Franca, A. Madureira, F. Valentin, Towards multiscale functions: enriching finite element spaces with local but not bubble-like functions, Comput. Methods Appl. Mech. Engrg. 194 (2005) 3006–3021.
[44] R. Araya, G. Barrenechea, F. Valentin, Stabilized finite element methods based on multiscale enrichment for the Stokes problem, SIAM J. Numer. Anal. 44 (2006) 322–348.
[45] D. Moser, J. Kim, N. Mansour, Direct numerical simulation of turbulent channel flow up to $Re_\tau = 590$, Phys. Fluids 11 (1999) 943–945.
[46] H. Choi, P. Moin, Effects of the computational time step on numerical solutions of turbulent flow, J. Comput. Phys. 113 (1994) 1–4.
[47] P. Gresho, R. Sani, Incompressible Flow and the Finite Element Method, Wiley, Chichester, 2000.
[48] R. Codina, Stabilized finite element approximation of transient incompressible flows using orthogonal subscales, Comput. Methods Appl. Mech. Engrg. 191 (2002) 4295–4321.
[49] V. Gravemeier, Variational multiscale large Eddy simulation of turbulent flow in a diffuser, Comput. Mech. 39 (2007) 477–495.
[50] V. John, G. Matthies, MooNMD – a program package based on mapped finite element methods, Comput. Visual Sci. 6 (2004) 163–170.
[51] V. Gravemeier, A consistent dynamic localization model for large Eddy simulation of turbulent flows based on a variational formulation, J. Comput. Phys. 218 (2006) 677–701.